Contrib. Plasma Phys. **46**, No. 7-9, 551 – 556 (2006) / **DOI** 10.1002/ctpp.200610043

A Finite Element Mesh in a Tokamak Edge Geometry

Y. Nishimura[*] and **Z. Lin**

Physics and Astronomy, University of California, Irvine, 92697-4575, USA

Received 19 October 2005, accepted 9 February 2006
Published online 22 August 2006

Key words Gyrokinetic poisson equation, finite element method, field aligned mesh.
PACS 52.55.Fa, 52.65.-y

A new finite element field solver is developed for gyrokinetic particle simulations in the tokamak edge. Introducing a simple analytical model for the edge geometry, our initial results of the finite element calculation is presented. An application of global field aligned mesh to the edge geometry is discussed.

1 Introduction

Due to a wide range of plasma parameters, anomalous plasma transport in the tokamak edge region is far from being understood. Within an extremely narrow radial range, different types of micro-instabilities can exist. At the H-mode pedestal, the ion temperature gradient exceeds the density gradient and induce instability known as the ion temperature gradient (ITG) mode. On the other hand, in the low temperature regions, the plasmas are collisional. In the low temperature regions, electrons are no longer adiabatic; resistive drift wave turbulence, [1] for example, can play an important role.

Conventionally, fluid simulation models are employed to study the turbulence dynamics in the edge. [2, 3] However, as known, the ion orbital size becomes comparable to the density and temperature scale length in the steep pressure region of H-mode plasmas. [4] Self-consistent kinetic turbulence simulation in the edge is highly in demand. As one of the preliminary work, in this paper, we present development of a finite element Poisson solver for gyrokinetic turbulence simulation in the edge. The solver can incorporate the non-adiabatic kinetic electron response.

For a large scale global gyrokinetic simulations, computational efficiency is a key issue. Global field aligned mesh [5] provides us with the highest efficiency without any approximation in geometry to describe the structure of the toroidal drift wave eigenmode. The field aligned mesh can be applied to the open-field-line regions as well, as long as the magnetic field is given by the Clebsch form $\mathbf{B} = \nabla\psi \times \nabla(\theta - \zeta/q)$ (here, ψ, θ, and ζ represent radial, poloidal, and toroidal labels, q is the safety factor). However, on the separatrix, the magnetic field line is purely toroidal at the X-point (takes infinite toroidal transits for the magnetic field line to reach there). Resultantly, the mesh points concentrate near the X-point. In this work, we apply the finite element elliptic solver [6] to analyze realistically how close we can approach to the separatrix. Since the main focus of this paper is the development of a mesh in the edge geometry for the gyrokinetic turbulence simulation, we do not consider the detailed phenomena in the tokamak edge plasmas. For example, plasma-wall interaction and the effects of neutrals are not referred to.

2 Differential form of gyrokinetic Poisson equation

In this section, we review the gyrokinetic Poisson equation to illustrate the importance of an elliptic solver. In global gyrokinetic simulations, in the GTC code [7] for example, an *iterative* Poisson solver [8] is employed assuming the adiabatic electron response. The iterative method is useful for global gyrokinetic simulations of

[*]Corresponding author: e-mail: nishimuy@uci.edu

toroidal plasmas, where the traditional spectral method is not applicable. However, with the inclusion of the non-adiabatic electron response, using either the split-weight schemes [9] or the hybrid model, [10] the iterative method is no longer applicable and the resulting gyrokinetic Poisson equation requires a new algorithm.

The general form of the gyrokinetic Poisson equation is in an integral form. [8, 11] Following Lee [11], the gyrokinetic Poisson equation is given by

$$\nabla^2\Phi - \frac{\tau}{\lambda_d^2}\left(\Phi - \tilde{\Phi}\right) = -4\pi e\left(\delta\bar{n}_i - \delta n_e\right) \tag{1}$$

where e is the unit charge, λ_d is the electron Debye length, $\delta\bar{n}_i$, δn_e are the ion and the electron guiding center charge density, and $\tau = T_e/T_i$ is the ratio between the equilibrium electron temperature T_e and the equilibrium ion temperature T_i. In Eq. (1), $\tilde{\Phi}$ is the second gyro-phase averaged potential. [11] From the ordering, [11] only the second term is retained, [8] giving Eq. (1) a form of an integral equation. To solve Eq. (1) numerically, an iterative double-gyro-averaging scheme is employed. [8] However, as noted above, the iterative method (under the integral form) cannot be applied for the non-adiabatic kinetic electrons. In the presence of non-adiabatic electrons, the inversion matrix of the iterative method cannot be diagonally dominant (see Appendix).

By expansion in the long wavelength limit, the second term of Eq. (1) becomes [11]

$$-\tau\lambda_d^{-2}\left(\Phi - \tilde{\Phi}\right) \sim \tau(\omega_{pi}/\Omega_i)^2\nabla_\perp^2\Phi, \tag{2}$$

where ω_{pi} is the ion plasma frequency and Ω_i is the ion cyclotron frequency. Instead, to calculate the response of the short wave length mode correctly, Padé approximation [12] is introduced on the right side of the gyrokinetic Poisson equation. [6] Normalizing Eq.(2) with ion gyro-radius for the length, the background density n_0, and T_e/e for the potential, we obtain

$$\nabla_\perp^2\Phi = -\left(1 - \frac{1}{\tau}\nabla_\perp^2\right)\left(\delta\bar{n}_i - \delta n_e\right). \tag{3}$$

Hereafter, we denote the right hand of Eq. (3) as "σ". Equation (3) will be employed for the gyrokinetic simulations in the presence of non-adiabatic kinetic electrons.

3 An analytical model for a tokamak edge geometry

Here we present a simple model, an analytical function to generate a tokamak edge like geometry. The model is given by a combination of circles and hyperbolic curves (see Fig.1). Although simple, it produces a geometry which is sufficient enough to study important edge turbulence issues. In particular, the model produces the X-point singularity [3, 5] of the divertor separatrix which is closely related to the application of the global field aligned mesh.

We consider a Hamiltonian of the form

$$H_c(x,y) = \frac{x^2}{2} + \frac{\left(y - \sqrt{2}\right)^2}{2} \tag{4}$$

(circles) for a domain which satisfies $y \geq x + \sqrt{2}$ and $y \geq -x + \sqrt{2}$, and

$$H_h(x,y) = \frac{x^2}{2} - \frac{y^2}{2} \tag{5}$$

(hyperbolic curves) for the rest of the domain. The center of the circle is located at $(x,y) = (0,\sqrt{2})$. Equations (4) and (5) apply to both the closed and open field line regions. Note $(x,y) \rightarrow (q,p)$, in terms of conventional canonical variables of classical mechanics. Corresponding equation of motions, $\dot{x} = \partial_y H$ and $\dot{y} = -\partial_x H$, are solved to obtain the trajectories on the $x-y$ plane. We employ the trajectories for the finite element mesh generation. Vertices are taken along the trajectories. Vertices are equally separated with respect to physically elapsed time [see Fig.1(b)]. As a result, the mesh points are separated in physically meaningful manner (equidistant in action-angle space). Here, the elapsed time corresponds to the magnetic field line pitch. The singular

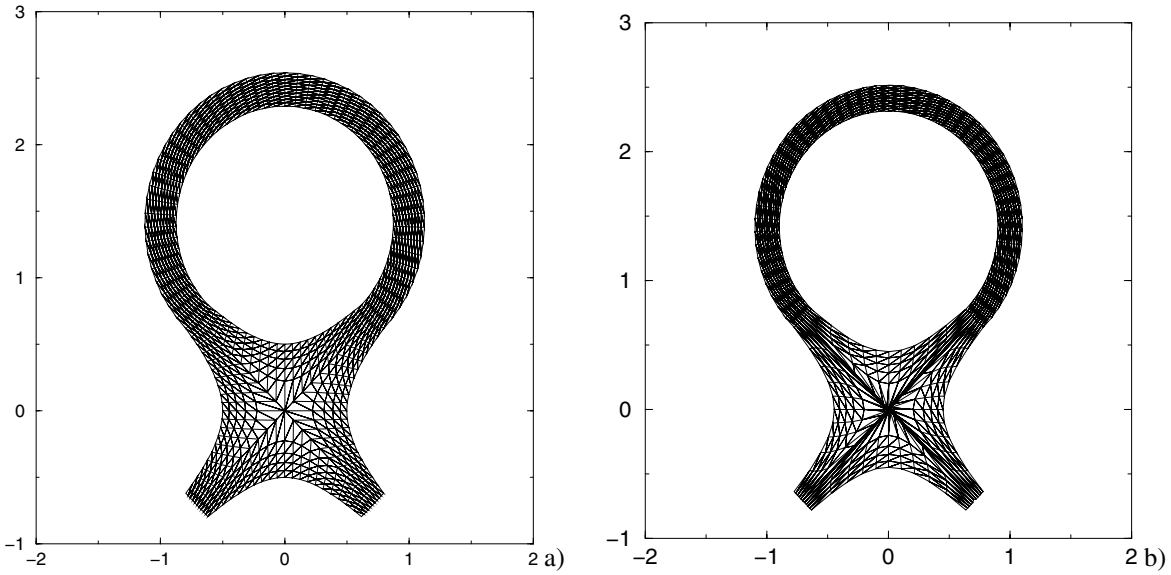

Fig. 1 Schematic diagram of (a) a regular mesh (equi-distant in x and y) and (b) a mesh with the X-point singularity (equi-distant in action-angle space). The singularity causes a problem in distorting the shape of the finite elements. Note the mesh size here is coarse for the illustration purpose.

feature of X-point singularity is already captured in Fig.1(b). The origin $(x, y) = (0, 0)$ or the X-point, behaves as a saddle point.

With Eqs. (4) and (5), we can obtain analytical solutions for the Poisson equation $\nabla_\perp^2 \Phi = \sigma$ (given the analytical form of Φ, we simply take the second derivative for σ). As one of the examples, we can choose Φ profile seen in typical H-mode plasmas. [13] The radial electric field E_r in H-mode plasmas can be represented by [14]

$$E_r = \frac{1}{n_0 Ze} \partial_r p_i - (\mathbf{V} \times \mathbf{B})_r \,, \tag{6}$$

where Z is the ion's charge number. When the Lorentz force term $(\mathbf{V} \times \mathbf{B})_r$ is less dominant, Eq. (6) gives an approximate relation $\Phi \sim -p_i$ (a parabolic rise, p_i is the ion pressure) inside the separatrix. On the other hand, the electric field in the scrape off layer is determined by the Bohm sheath dynamics. Contrary to the regions inside the separatrix, we obtain an approximate relation $\Phi \sim T_e$ (a parabolic drop). Such equilibrium electrostatic potential can be given by

$$\Phi(r) = \frac{1}{w^2}(r - r_s - w)^2 \tag{7}$$

where $r^2 = x^2 + (y - \sqrt{2})^2$, r_s is the radius of the circle on the separatrix ($r_s = 1$ for our specific case), and w is the width of the simulating domain. Imposing Φ values on each flux surface [15] to be constant, we obtain a surprisingly simple form

$$\sigma(x, y) = \nabla_\perp^2 \Phi = \frac{2}{w^2}(x^2 + y^2) \tag{8}$$

in the hyperbolic region [in the circle region, simply $\sigma = r^{-1}\partial_r(r\partial_r\Phi)$].

4 Numerical solution from a finite element elliptic solver

In general, the finite element (FE) method [16] is suitable for dealing with complicated geometries, where unstructured meshes are employed. For the core turbulence study, recently an FE Poisson solver is developed and

successfully implemented to a gyrokinetic particle simulation. [6] In the edge, since the radial variation of the element areas are small, we restrict ourselves to logically rectangular mesh in this paper (note the difference from core turbulence simulation [6] where a logically non rectangular mesh is employed). In the finite element method, the main task is to relate the vertex indices to the element indices (triangles as in Fig.1). Once the indices are related, the rest of the task is to solve a linear matrix equation "$A\Phi = \sigma$" which generally is a large sparse matrix. [16] In this work, we employ state of the art PETSc (Portable, Extensible Toolkit for Scientific Computation) code to solve the matrix. [17] Using PETSc for the core turbulence simulation, an optimistic CPU timing is obtained up to a million mesh points per poloidal plane.

An example of the numerical solution of Φ profile is shown in Fig.2 as a radial cut at the top ($x = 0$ and $2.274 > y > 2.474$) of the simulating domain [see Fig.1(b)]. For this example, $\sigma = 1.0 = const$ is taken, being consistent with the parabolic profile seen in Fig.2. A homogeneous Dirichlet boundary condition is taken and incorporated into the matrix equation. Here the total number of the vertices is 14342, giving rise to 96072 nonzero components in a 14342×14342 sparse matrix. Note in the type of the meshes as Fig.1(b) there are no mesh points exactly on the separatrix. We avoid to do so because of the X-point singularity. The last closed flux surface and the first open surface are chosen so that they are separated by an order of ion gyroradius. The two surfaces are connected to produce the finite element mesh.

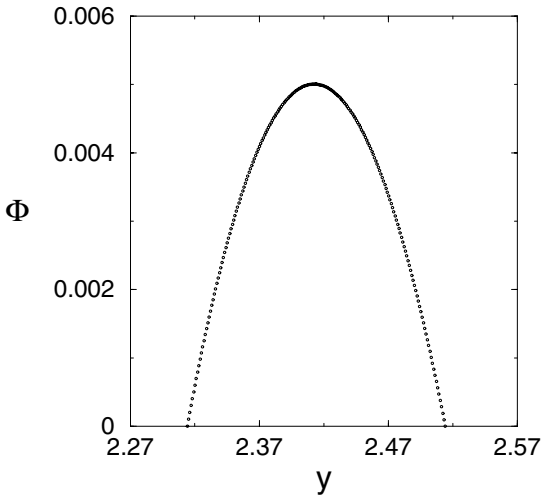

Fig. 2 Radial profile of the solutions Φ at the top ($x = 0$ and $2.274 > y > 2.474$) of the simulating domain in Fig.1(b).

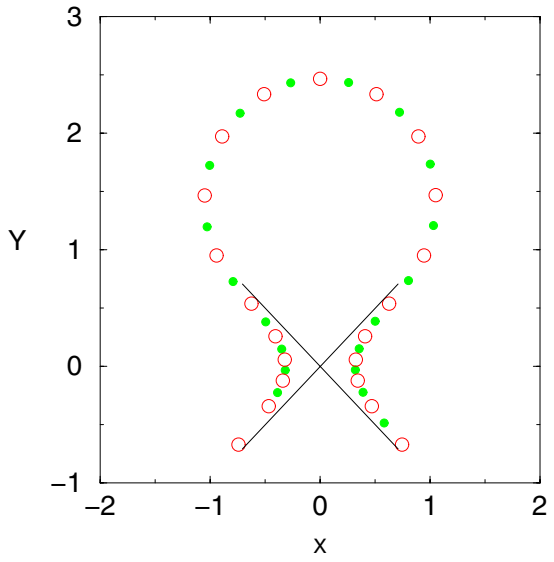

Fig. 3 A method of generating the field aligned mesh in the open field line region. Red is the mesh at the toroidal angle $\zeta = 0$ and green (filled) is at $\zeta = \pi$. The mesh points are forwarded clock wise in terms of elapsed time. Demonstrated on one flux surface. For a contrast, the separatrix is given by solid black lines.

In global gyrokinetic simulations, [7] the field aligning [5] is an indispensable tool (if the mesh is not field aligned one needs to take ~ 100 times larger mesh points in the toroidal direction). The global field aligned mesh takes the advantage of helically twisted magnetic field lines in capturing resonant modes on each flux surface (note, integrable good flux surfaces are presumed in constructing the global field aligned mesh; we do not study magnetic stochasticity, for example ergodic divertors [18]). The mesh rotates together with the equilibrium magnetic field lines and is not symmetric in the toroidal direction. Further, since $q(r)$ in general is not constant, the flux surfaces do not rotate rigidly. A method of generating global field aligned mesh in the open field line region is illustrated in Fig.3. In practice, we forward the chain of mesh points corresponding to the q profile on each flux surface. In the example of Fig.3, red circles correspond to mesh points at the toroidal angle $\zeta = 0$ and green filled circles at $\zeta = \pi$. Although the number of vertices should be increased by a factor of one on the $\zeta \neq 0$ planes (since the red mesh points on the "divertor plates" need to move), the application of the finite element

method is straightforward. Note, in applying the form of Eqs.(4) and (5), one needs to match the pitch at the connection points (that are along $y = \pm x + \sqrt{2}$). The velocity of the trajectories (how fast the mesh points move along flux surface; varies even on one surface) is given by $v = (\dot{x}^2 + \dot{y}^2)^{1/2}$, which is $v_c = (x^2 + y^2)^{1/2}$ in the circle region and $v_h = [x^2 + (y + \sqrt{2})^2]^{1/2}$ in the hyperbolic region.

5 Summary and discussions

In this work, a new finite element field solver is developed and applied to a tokamak edge geometry. The field solver enables studying non-adiabatic kinetic electrons and electromagnetic effects in the global gyrokinetic simulations. We have presented a simple analytical model for the edge divertor geometry. The analytical model can be useful in the initial phase of the edge gyrokinetic code development if we are to apply particle simulations in the edge (compared to numerical equilibrium from Grad Shafranov solver, which may obscure mathematical singularity of the separatrix and the X-point). The mesh generation we presented in this paper is no more than a proto-type. For example, in the particle in cell simulations, the number of particles per cell should be kept nearly constant (thus we prefer to keep the area of the elements to be constant). At the same time, from the standpoint of turbulence vortex dynamics, we should keep the element shape isotropic (the y-x mesh size ratio should not be larger than two). [2] All these processes in refining the mesh remain as our near term future work.

Acknowledgements One of the authors Y.N. thank Dr. Taik-Soo Hahm and Dr. Mark Adams for useful comments. This work is supported by Department of Energy (DOE) Cooperative Agreement No. DE-FC02-04ER54796 and 06ER54860.

A Iterative method in the presence of non-adiabatic electrons

Let us consider a normalized gyrokinetic Poisson's equation

$$\Phi - \tilde{\Phi} = \delta n^{(ion)} - \delta n^{(electron)}$$

in a Cartesian grid. Here, $\tilde{\Phi}$ is the second gyro-phase averaged potential [11] as in Eq. (1). The nine point scheme for the double gyro averaging (by Lin and Lee [8]) is given by

$$\tilde{\Phi_{i,j}} = \frac{1}{16}\left(4\Phi_{i,j} + 2\Phi_{i\pm2,j} + 2\Phi_{i,j\pm2} + \Phi_{i\pm2,j\pm2}\right)$$

Here, the subscripts i and j are for the x and y grid indices, respectively. If electrons are adiabatic we have

$$2\Phi_{i,j} - \tilde{\Phi_{i,j}} = \left(2 - \frac{4}{16}\right)\Phi_{i,j} - \frac{1}{16}\left(2\Phi_{i\pm2,j} + 2\Phi_{i,j\pm2} + \Phi_{i\pm2,j\pm2}\right) = \delta n_{i,j}^{(ion)}$$

If non-adiabatic [without using $\Phi = \delta n^{(electron)}$] we have

$$\Phi_{i,j} - \tilde{\Phi_{i,j}} = \frac{1}{16}\left(12\Phi_{i,j} - 2\Phi_{i\pm2,j} - 2\Phi_{i,j\pm2} - \Phi_{i\pm2,j\pm2}\right) = \delta n_{i,j}^{(ion)} - \delta n_{i,j}^{(electron)} \tag{9}$$

For linear iterative method $A \cdot \Phi = \sigma$ to converge, the matrix need to be diagonally dominant. Denoting a_{ij} as the components of the matrix A,

$$\max_i \left[\sum_{j=1, i\neq j} \left|\frac{a_{ij}}{a_{ii}}\right|\right] < 1.$$

For the adiabatic electron case the left side of Eq.(3) will be $(3/4)/(7/4) = 3/7 < 1$, while $(3/4)/(3/4) = 1$ for the non-adiabatic electron case. It is worth pointing out there are ongoing efforts [19, 20] to solve Eq. (9) directly by constructing a matrix [the matrix is much more dense than that obtained from Eq. (3) and the finite element method, and thus the matrix inversion takes much longer computational time]. Further intensive work in speeding up the matrix inversion is required (algebraic multigrid method, [21, 22] for example) if one intends to apply the latter method (the direct matrix inversion) for the mesh size corresponding to realistic tokamak experiments.

References

[1] F.F. Chen, *Introduction to Plasma Physics and Controlled Fusion*, 2nd ed. (Plenum Press, New York, 1983), p.218.
[2] B. Scott, Phys. Plasmas **7**, 1845 (2000).
[3] X.Q. Xu, R.H. Cohen, T.D. Rognlien, and J.R. Myra, Phys. Plasmas **7**, 1951 (2000).
[4] F. Wagner et al., Phys. Rev. Lett. **49**, 1408 (1982).
[5] B. Scott, Phys. Plasmas **5**, 2334 (1998).
[6] Y. Nishimura, Z. Lin, J.L.V. Lewandowski, and S. Ethier, J. Comput. Phys. **214**, 657 (2006).
[7] Z. Lin, T. Hahm, W. Lee, W. Tang, and R. White, Science **281**, 1835 (1998).
[8] Z. Lin and W.W. Lee, Phys. Rev. E **52**, 5646 (1995).
[9] W.W. Lee et al., Phys. Plasmas **8**, 4435 (2001).
[10] Z. Lin and L. Chen, Phys. Plasmas **8**, 1447 (2001).
[11] W.W. Lee, J. Comput. Phys. **72**, 243 (1987).
[12] T.S. Hahm and L. Chen, Phys. Fluids **28**, 3061 (1985).
[13] T.D. Rognlien, D.D. Rytov, N. Mattor, and G.D. Porter, Phys. Plasmas **6**, 1851 (1999).
[14] F.L. Hinton and Y.-B. Kim, Nucl. Fusion **34**, 899 (1994).
[15] In this paper, we use the term flux surface to represent each curve on different radial locations. In the closed magnetic field line region, the flux surface literally corresponds to the physical one.
[16] K.H. Huebner, D.L. Dewhirst, D.E. Smith, and T.G. Byrom, The Finite Element Method for Engineers, 4th ed. John Wiley & Sons, New York, 2001, p. 43.
[17] Portable extensible toolkit for scientific computation; www-unix.mcs.anl.gov/petsc.
[18] A.M. Runov, D. Reiter, S.V. Kasilov, M.F. Heyn, and W. Kernbichler, Phys. Plasmas **8**, 916 (2001).
[19] Y. Nishimura, Z. Lin, M.F. Adams, D.E. Keyes, W.W. Lee, and J. Manickam, Bull. Am. Phys. Soc. **50** (8), 351 (2005).
[20] A. Mishchenko, A. Könies, and R. Hatzky, Phys. Plasmas **12**, 062305 (2005).
[21] V.E. Henson and U.M. Yang, Applied Numerical Mathematics **41**, 155 (2002).
[22] *hypre*: high performance preconditioners; Scalable Algorithms Group, Center for Applied Scientific Computing, http://www.llnl.gov/CASC/hypre.

